S. Funahashi (Ed.)

Representation and Brain

S. Funahashi (Ed.)

Representation and Brain

With 101 Figures, Including 28 in Color

Springer

Shintaro Funahashi, Ph.D.
Professor, Kyoto University Kokoro Research Center
Yoshida-Honmachi, Sakyo-ku, Kyoto 606-8501, Japan

ISBN 978-4-431-73020-0 Springer Tokyo Berlin Heidelberg New York

Library of Congress Control Number: 2007931333

Printed on acid-free paper

Springer is a part of Springer Science+Business Media
springer.com

Typesetting: SNP Best-set Typesetter Ltd., Hong Kong
Printing and binding: Kato Bunmeisha, Japan

Preface

In our daily life, we perceive a variety of stimuli from the environment. However, among these, only a few selected stimuli are further processed in our brain. These selected stimuli are processed and integrated together with the information stored in long-term memory to generate an appropriate behavior. To achieve these processes, the brain needs to transform a variety of information into specific codes to be able to process it in the nervous system. For example, a digital computer uses a binary code to process information. A variety of information is transformed into a combination of 1's and 0's, or "on" and "off" states. When we push the "A" key on the keyboard, the character "a" appears on the monitor. In this case, the information that an "A" key was pushed is transformed into the binary code 01100001 in the computer, and this binary code is used to present the character "a" on the monitor. When we push the "A" key together with the "shift" key, however, this information is transformed into the binary code 01000001, and this code is used to present the character "A" on the monitor. Different characters and symbols are assigned to different binary codes in the computer using a specific common rule (e.g., ASCII format). A variety of information processed in the computer is represented using the specific rules of the binary code. This enables convenient and efficient use of any computer for a variety of purposes. By understanding the rules of information processing and the codes to represent information, we can understand how the computer works and how the computer processes information.

Similarly, specific common rules or common methods of coding can also be used in the brain for processing and representing information. How information is represented in the nervous system and how information that is represented in the nervous system is processed are the most important factors for understanding brain functions, especially for understanding neural mechanisms of higher cognitive functions such as thinking, reasoning, judging, and decision making. These subjects are the main themes of this book, in which we have tried to show the current state of our knowledge regarding information representation in the nervous system. We approach these subjects from four directions: studies on visual functions (Part I), motor functions (Part II), memory functions (Part III), and prefrontal cortical functions (Part IV).

How stimuli in our environment are represented in the nervous system is best known in the visual system. ***Part I*** focuses on this subject, particularly in visual information processing and visual image production. Perception of a visual target and neural responses to the target are strongly influenced by the context surrounding the target. The specific layout of the features surrounding the target can produce either a suppressive or a facilitatory effect on neural responses to the target. Ejima et al. investigated contextual effects of meta-contrast masking, chromatic induction, and the contour processing in the perception of an occluded object in human visual areas using fMRI. Brain activity in the higher-order visual areas showed more prominent specificity to stimulus attributes and contexts. Ejima et al. discuss this contextual modulation together with the possibility that the modulation plays different roles in different processing stages. By contrast, most theories of visual perception employ the concept of "top-down processing" (TDP). However, this concept has not been articulated in detail, and usually the term is used to indicate any use of stored knowledge in vision. Using data from a variety of research fields, Ganis and Kosslyn propose four distinct types of TDP (reflexive processing, strategic processing, threshold lowering, and completion) that are engaged in different circumstances. They showed that *reflexive processing* occurs when bottom-up information automatically triggers TDP, which in turn sends feedback to an earlier process. *Strategic processing* occurs when executive control processes are used to direct a sequence of operations. *Threshold lowering* occurs when TDP increases the sensitivity of a neural population. Finally, *completion* occurs when TDP fills in missing information.

The neural mechanism of invariant object and face recognition is a major computational problem that is solved by the end of the ventral stream of the cortical visual pathway in the inferior temporal cortex. The formation of invariant representation is crucial for the areas that receive information from the inferior temporal cortex, so that when they implement learning based on one view, size, and position on the retina of the object, the learning is generalized later when the same object is seen in a different view, size, and position. Rolls presents evidence that invariant representations are provided by some neurons in the inferior temporal cortex and hypothesizes about how these representations are formed.

To efficiently interact with the environment, not only perception of objects and scenes but also maintenance of these visual representations for a brief period is crucial. Saiki focuses on some of the important issues regarding visual working memory for objects, scenes, and capacity; representational format (in particular feature binding); and manipulation of memory representations. Based on findings from both behavioral and functional brain imaging experiments, Saiki describes working memory for objects and scenes as a network of specialized brain regions.

Motor imagery and body schema are also good examples for understanding how information is represented in the nervous system. The “mirror neuron system” is an especially good model for understanding how we construct motor imagery and body schema and how we perceive and understand actions made by

others. ***Part II*** focuses on this subject. Recent neuroanatomical and functional data indicate that action itself and perception of action are linked, and that this link occurs through reciprocal parietofrontal circuits. These circuits not only are involved in different types of sensory-motor transformations but also allow the emergence of cognitive functions such as space perception and understanding an action. The representation of the goal of the action at the single neuron level is fundamental for these functions, because it constitutes internal knowledge with which the external word is matched. The mirror neuron system is an example of a neural mechanism through which we can recognize and interpret actions made by others by using our internal motor repertoire. Fogassi examined several types of motor functions, with a particular emphasis on those functions based on the mirror system, such as action understanding, understanding of intention, and imitation. Similarly, Murata describes the mirror system in the parietal cortex as possibly having a role in monitoring self-generated action by integrating sensory feedback and an efference copy. This idea is based on data showing that the parietal cortex receives somatosensory and visual inputs during body action, and that matching the efference copy of the action with the visual information of the target object is performed in the parietal area AIP (anterior intraparietal area).

The brain creates the neural representation of the motor imagery and the body schema by integrating motor, somatosensory, and visual information. Naito examined the neural representation of the motor imagery for hand movements using motor illusions, and showed that the execution, mental simulation, and somatic perception related to a particular action may share a common neural representation that uniquely maps its action in action-related areas in the human brain.

In addition to hand or arm movements, eye movements also play significant roles in our daily life. One of the most fundamental decisions in human behavior is the decision to look at a particular point in space. Recent advances in recording neural activity in the brain of epileptic patients have made it possible to identify the role of the brain areas related to the control of eye movements. Freyermuth et al. summarize some of the brain imaging studies on cortical control of saccades and describe recent findings obtained with intracranial recordings of brain activity in epileptic patients. They particularly focus on the subject of decision making in saccadic control by describing experiments during which subjects decide to make a saccade toward a particular direction in space.

Understanding how information is stored as memory in the brain is also a way to understand how a variety of information is represented internally in the nervous system. In order to discuss memory, we need to solve some important questions regarding representation, such as how the information is stored in the brain, what mechanism controls memory representation, and how flexible memory representation is. ***Part III*** focuses on this subject.

Examining the characteristics of the activity of place cells is one way to understand how flexible memory representation is. Brown and Taube examined whether place fields of hippocampal CA1 place cells are altered in animals receiving lesions in brain areas containing head direction (HD) cells. Although place

cells from lesioned animals did not differ from controls on many place-field characteristics, the signals (outfield firing rate, spatial coherence, and information content) were significantly degraded. Surprisingly, place cells from lesioned animals were more likely modulated by the directional heading of the animal. These results suggest that an intact HD system is not necessary for the maintenance of place fields, but lesions in brain areas that convey the HD signal can degrade this signal.

Sakurai explains why ensemble coding by cell assembly is a plausible view of the brain's neural code of memory and how we can detect ensemble coding in the brain. To consider ensemble coding, partial overlap of neurons among cell assemblies and connection dynamics within and among the assemblies are important factors. The actual dynamics include dependence on types of information-processing in different structures of the brain, sparse coding by distributed overlapped assemblies, and coincidence detection as a role of individual neurons to bind distributed neurons into cell assemblies. Sakurai describes functions of these parameters in memory functions.

Numbers are indispensable components of our daily life. We use them to quantify, rank, and identify objects. The verbal number concept allows humans to develop superior mathematical and logic skills, and the basic numerical capability is rooted in biological bases that can be explored in animals. Nieder describes its anatomical basis and neural mechanisms on many levels, down to the single-neuron level. He shows that neural representations of numerical information can engage extensive cerebral networks, but that the posterior parietal cortex and the prefrontal cortex are the key structures for this function in primates.

Finally, thinking is one of the most important subjects in the field of cognitive neuroscience. Thinking can be considered as neural processes in which a variety of internally representing information is processed simultaneously to produce a particular product in a particular context. Therefore, understanding how internally representing information is processed and how new information is created from representations being maintained in the nervous system must be the way to understand the neural mechanism of thinking. The prefrontal cortex is known to participate in this mechanism. Therefore, in ***Part IV***, prefrontal functions are examined in relation to the manipulation and processing of internal representation.

An important function of the prefrontal cortex is the control and organization of goal-directed behavior. Wallis examines neural mechanisms underlying this function. This mechanism can be grouped in several levels according to the level of abstraction. At the simplest level, prefrontal neurons represent the expected outcomes of actions directed toward basic goals of homeostatic maintenance (e.g., maximizing energy intake or minimizing energy expenditure). At a more complex level, prefrontal neurons encode representations of arbitrary relationships between specific sensory stimuli and specific actions. Finally, at the most abstract level, prefrontal neurons represent rules and concepts. Wallis describes how these representations ensure optimal action selection for organisms.

The dorsolateral prefrontal cortex is known to participate in working memory. Working memory is a fundamental mechanism for many cognitive processes including thinking, reasoning, decision making, and language comprehension. Therefore, understanding neural mechanisms of working memory is crucial for understanding neural mechanisms of these cognitive processes. Funahashi describes experimental results showing the temporal change of information represented by a population of prefrontal activities during performances of spatial working memory tasks. He also points out widespread functional interactions among neighboring neurons and the dynamic modulation of functional interactions depending on the context of the trial, and concludes that functional interactions among neurons and their dynamic modulation depending on the context could be a neural basis of information processing in the prefrontal cortex.

Cognitive functions could be an outcome of the complex dynamic interaction among distributed brain systems. McIntosh describes two emerging principles which may help guide our understanding of the link between neural dynamics and cognition. The first principle is neural context, where the functional relevance of a brain area depends on the status of other connected areas. A region can participate in several cognitive functions through variations in its interactions with other areas. The second principle states that key nodes in distributed systems may serve as "behavioral catalysts," enabling the transition between behavioral states. McIntosh suggests that an area either facilitates or catalyzes a shift in a dominant pattern of interactions between one set of regions to another, resulting in a change in the mental operation by virtue of its anatomical connections.

Thus, in this book, readers will find the current state of our knowledge regarding information representation in the nervous system. An analysis of single-neuron activity recorded from behaving animals has been used to reveal rules and codes that are used in the nervous system. We now know how light with a particular wave length is represented at the single-neuron level in the retina, the primary and secondary visual areas, and the inferior temporal cortex. We also know how the preparation of the movement toward a particular direction is represented in the activity of motor and premotor neurons. Advancement in neuroimaging techniques and the usage of a variety of behavioral paradigms in combination with advanced neurophysiological techniques will make it possible to approach these issues more closely.

I would like to express many thanks to the contributors of this book. I also would like to acknowledge that this publication is supported by the 21st Century COE (Center of Excellence) program of the Japanese Ministry of Education, Culture, Sports, Science, and Technology (MEXT) (Program number D-10, Kyoto University).

Shintaro Funahashi
Kyoto University
Kyoto, Japan

Contents

Part I
Visual Information Processing and Visual Image Production

1
Visual Perception of Contextual Effect and Its Neural Correlates

Yoshimichi Ejima[1], Shigeko Takahashi[2], Hiroki Yamamoto[3], and Naokazu Goda[4]

1. Introduction

Gestalt principles of grouping, that is, how local signals are integrated across space to generate global percepts, have been central to the study of vision. Traditionally, visual information has been seen as ascending through a hierarchy of cortical areas, with cells at each successive stage processing inputs from increasingly larger regions of space. However, recent research using neurophysiological recordings in animals and functional magnetic resonance imaging (fMRI) in humans makes it increasingly clear that this traditional view is overly simplistic. The long-distance integration of visual signals can occur in the very early stages of processing. The response of cells in the primary visual cortex (V1) to stimulation of their receptive field can be modulated in a selective way by contextual stimuli lying far outside the receptive field in the receptive field surround. Although there is unquestionably some degree of serial processing from V1 to higher cortical areas, in many situations, activity in the early visual cortex is better correlated with, and may be more intimately involved in, perception than activity in later areas. Identifying the neural circuitry underlying these long-distance computations is crucial, because they may represent the neural substrates for feature grouping and figure-ground segregation. Here, in the first section, we have addressed this question by studying the cortical processing of simultaneous contrast effect of grating patterns by fMRI measurement.

Whether perceptual grouping operates early or late in visual processing is an ongoing problem. One hypothesis is that elements in perceptual layouts are grouped early in vision, by properties of the retinal image, before meanings have

[1]Kyoto Institute of Technology, Matsugasaki, Sakyo-ku, Kyoto 606-8585, Japan
[2]Department of Fine Arts, Kyoto City University of Arts, 13-6 Ohe-Kutsukake-cho, Nishikyo-ku, Kyoto 610-1197, Japan
[3]Graduate School of Human and Environmental Studies, Kyoto University, Yoshida-nihonmatsu-cho, Sakyo-ku, Kyoto 606-8501, Japan
[4]National Institute for Physiological Sciences, 38 Aza-saigou-naka, Myoudaiji-cho, Okazaki, Aichi 444-8585, Japan

been determined. Another hypothesis is that perceptual grouping operates on representation in higher cortical areas. How can early grouping be operationally defined and distinguished from higher-level grouping? To examine this question, we investigated grouping relative to meaning (see third section). By examining grouping relative to ambiguous achromatic display, we have demonstrated that perceptual grouping is based on the activation of early visual areas as well as on the activity of prefrontal cortical areas. This result permits the integration of cortical activity in early and higher cortical areas with regard to grouping by meaning.

2. Spatiotemporal Cortical Map of Contextual Modulation in the Human Early Visual Area

The appearance of a stimulus varies depending on the context in which the stimulus is presented. For instance, perceptual contrast of a stimulus is, in a complicated fashion, affected by surrounding stimuli depending on the relative contrast, orientation, and direction between the stimulus and the surround (Cannon and Fullenkamp 1991; Ejima and Takahashi 1985; Takeuchi and DeValois 2000; Xing and Heeger 2000). These lateral interaction effects, recently often called contextual effects, raised a fundamental question: how does local information interact to generate a percept across retinotopic space? It has been proposed that lateral interaction beyond "classical" receptive field in early visual areas is involved in complex functions such as contrast normalization and pop-out and figure-ground segregation (Kastner et al. 1997; Knierim and van Essen 1992; Lamme 1995; Sillito et al. 1995; Zipser et al. 1996).

Recent neuroimaging studies have demonstrated analogous, orientation-tuned lateral interaction in humans; responses to a local stimulus in early human visual areas were suppressed by adding surround stimuli (Kastner et al. 1998, 2001; Ohtani et al. 2002; Zenger-Landolt and Heeger 2003). However, the detailed spatial properties of the lateral interaction remain unclear. The spatial properties are important characteristics because they help to constrain the mechanism generating the modulation. The modulation may result from multiple mechanisms: long-range interaction, a short-range mechanism, and a mechanism sensitive to the local feature contrast at the boundary (Kastner et al. 1997; Knierim and van Esses 1992; Reinolds 1999; Sillito et al. 1995).

Here, we have analyzed the spatial distribution of response modulation in the human visual area during contextual change in perceptual contrast using a new fMRI analysis and visualization technique. Visual stimuli were composed of two test gratings or a circular surround grating or both (Fig. 1a). Stimuli were composed of test gratings in the two quarter (mainly upper right and lower left) visual fields at the middle eccentricities (2°–10°) and/or a large surround grating (0°–15° eccentricity), presented on a uniform gray background with a small fixation point. The test and surround gratings were spatially separated by small gaps. The orientations of the gratings were changed pseudo-randomly at 1 Hz (22.5°, 77.5°,

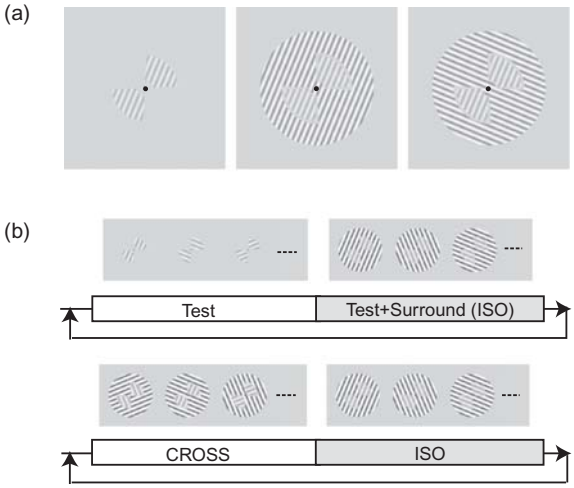

FIG. 1. Example stimuli. **a** Stimulus consisted of a test component (two test gratings located at 2°–10° eccentricities in the upper right and lower left visual field) and surround component (a circular grating subtending to 15° eccentricity) separated from the test by small gaps. *Left*, test component only; *center*, iso-orientation stimulus (test plus iso-oriented surround); *right*, cross-orientation stimulus (test plus cross-oriented surround). The test gratings are perceived as lower contrast, especially in the presence of iso-oriented surround (*center panel*). **b** Experimental protocol. In each scan session, two different types of stimuli (*top*, test-only and iso-orientation; *bottom*, cross- and iso-orientation) were presented repeatedly in alternating 16-s blocks. The orientations of the test and surround gratings were changed within a block pseudo-randomly at 1 Hz

–22.5°, or –77.5°). Only oblique orientations were employed to avoid an "oblique effect" in fMRI response (Furmanski and Engel 2000). When the test and surround gratings were presented simultaneously, their relative orientation was kept constant at 0° (iso-orientation) or 90° (cross-orientation). Luminance contrast (0% [absence], 40%, or 80%), spatial frequency (2.0 cpd (cycle per degree) or 0.66 cpd), and relative spatial phase (0° or 180°) of the test and surround gratings were also manipulated. In the reference scan condition, a stimulus with the test component only (80% contrast, 2.0 cpd) and that with a surround component only (80% contrast, 2.0 cpd) were used. Retinotopic mapping experiments (Engel et al. 1994; Sereno et al. 1995) were also employed to locate visual areas for each subject. A checkered ring (2° width), expanding from the central (0.75°) to peripheral (16°), was used to map eccentricity in the visual field. A checkered 45° wedge, rotating counterclockwise, was used to map angular positions in the visual field. Subjects were instructed to stare continuously at the fixation point and to press a photo switch when the ring appeared at the center or at horizontal and vertical meridians to retain visual awareness.

Anatomical and functional MR measurements were conducted with a standard clinical 1.5-tesla scanner (General Electric Signa, Milwaukee, WI, USA) with echoplanar capability (Advanced NMR, Wilmington, MA, USA). Functional volumes were realigned (Woods et al. 1992). The functional volumes were then coregistered to the standard structural volume and thus to the reconstructed cortical surface. From the standard structural volume, the cortical surface was reconstructed for each hemisphere (Ejima et al. 2003). The retinotopic areas were determined by analyzing data from fMRI scans using phase-encoded stimuli. The boundaries between the areas V1d, V1v, V2d, V2v, V3, VP, and V4v were determined based on the retinotopic criteria reported in previous studies (Ejima et al. 2003; Engel et al. 1994, 1997; Sereno et al. 1995).

The fMRI time series were sampled from each retinotopic area (V1d, V1v, V2d, V2v, V3, and VP). First, the surface regions of retinotopic areas defined by retinotopic mapping were inflated to 3-mm thickness, taking into account the thickness of gray matter, giving the gray matter regions of interest (GOIs). Next, the fMRI time series of the voxels overlapping with each GOI were sampled separately. The sampled voxel time series were then high-pass filtered to remove linear and nonlinear trends and converted to units of percent signal.

The fMRI time series sampled for each retinotopic area were then analyzed on the basis of the representation of eccentricity of the visual field. First, a set of "bands" was defined on the reconstructed surface based on the geodesic distance (the distance of the shortest path along the cortical surface) from the peripheral limit of the eccentricity map (16°) to the foveal region in each area. The bands were delineated so that the center of the bands differed in 1.5-mm steps in cortical distance and the width of each band was 3 mm. Thus, each band overlapped adjacent bands. We called these bands "iso-eccentricity bands." Next, the voxel time series within each band were averaged, giving the mean time series of each eccentricity. Hereafter, the mean time series from repeated scans were averaged. The time series of each eccentricity were further averaged across stimulus cycles of the stimuli (24 or 48 cycles of two 16-s blocks). The event-related responses of different eccentricities were displayed as a spatiotemporal cortical map using an iso-contour plot with an interpolated pseudo-color format.

2.1. Surround Suppression

2.1.1. Retinotopic Localization of Stimulus Components

We first identified retinotopic subregions responding to a test stimulus component (located in the lower left and upper right quadrants of the visual field) and its surround stimulus components in each retinotopic area. Because the test and surround components were located at different eccentricities in the quarter visual fields, the regions responding to these components could be separated effectively in terms of retinotopy of the visual field eccentricity in each area. Figure 2a shows the results for right V1d, V2d, and V3, which represent the lower left quadrant of the visual field (Fig. 2, left panel) for one subject. These plots represent the

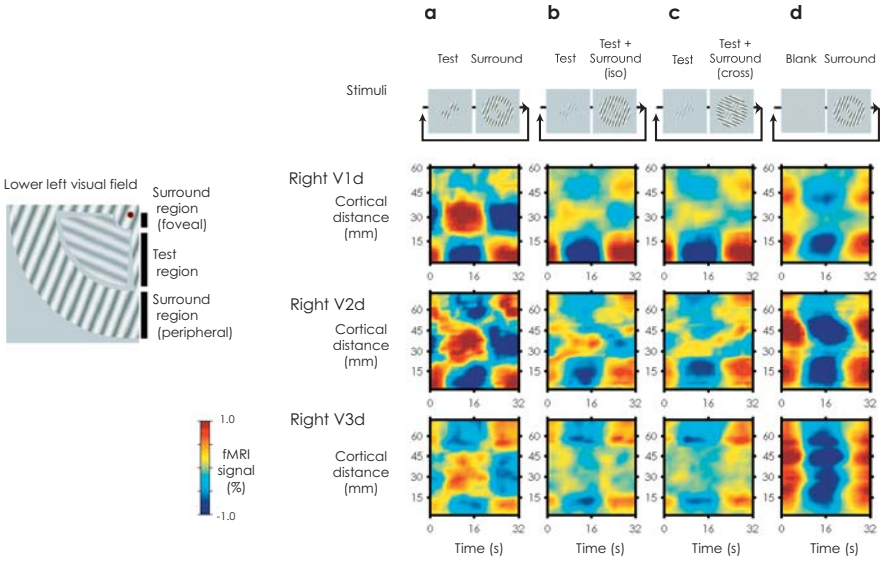

FIG. 2. Spatiotemporal maps of right V1d, V2d, and V3 for one subject. In each panel, mean time course at different eccentric locations for a stimulus cycle (two 16-s blocks) is plotted in pseudo-color format. The eccentric location was represented by cortical distance from a 16° eccentricity line. Increasing the distance (from lower to upper on *vertical axis*), the eccentricity varies from periphery to fovea. Schematic illustrations of the lower left visual field of stimuli in the two blocks are shown on the left of the pseudo-color plots. **a** Results for test-surround alternation (localizer condition). **b** Results for presenting an iso-oriented surround with a test component (iso-oriented surround condition). **c** Results for presenting a cross-oriented surround with a test component (cross-oriented surround condition). **d** Results for presenting an iso-oriented surround without test component (control condition). fMRI, functional magnetic resonance imaging

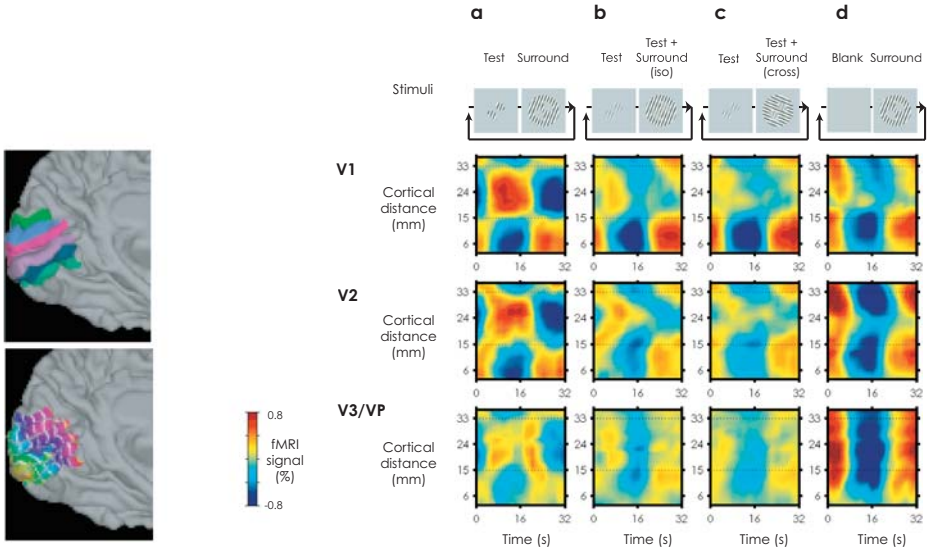

FIG. 3. Spatiotemporal maps of V1, V2, and V3/VP, computed by averaging across hemispheres (right dorsal and left ventral). The *dotted lines* represent the test/surround boundaries, which were determined from the results of localizer scans

spatiotemporal modulation of fMRI response concisely. Each horizontal trace represents the mean time course of an iso-eccentricity band, whose location is represented by the cortical distance (from peripheral to foveal region). Colors denote the signal values of the blood oxygen-action level-dependent (BOLD) contrast. These plots clearly show that the fMRI responses in middle eccentricities (about 15 mm wide) increased after presentation of the test with a hemodynamic delay, and those in more foveal and peripheral regions increased after the surround presentation. The spatial regions responding to the test were clearly separated from those of the surround.

We then averaged the spatiotemporal maps across subjects and hemispheres to improve signal-to-noise ratio further (Fig. 3a). As the extent of each area on the cortical surface was significantly different across subjects and hemispheres, we coregistered the map of each area before averaging so that the boundaries of the test and surround regions matched their average cortical distances using linear interpolation. To make averaged maps for each visual area V1, V2, and V3/VP, maps of the right dorsal and left ventral parts for two subjects were averaged.

2.1.2. Effect of Adding Iso- and Cross-Oriented Surround

Using similar stimulus setups and analysis, we examined how the response to the test component varied when the surround component was presented simultaneously. The test (40% contrast) was continuously presented during alternating two blocks. The high contrast surround (80% contrast, the same spatial phase as the test phase) was presented in only one of the two 16-s blocks. Because the test was always presented, any variation in the response was attributed to the effects by surround stimulation. We used two types of surround stimuli: an "iso-oriented" and a "cross-oriented" surround. In these stimuli, the relative orientation of the test and surround gratings was kept constant at either 0° (iso-orientation) or 90° (cross-orientation), while each orientation of the test and surround was changed at 1 Hz. Observers reported that the test was perceived as a lower contrast in the presence of the surrounds and the contrast suppressions were stronger for iso- than cross-orientation stimuli.

The pattern of the results indicated that the iso- and cross-oriented surround suppressed the test response in at least V1 and V2. In individual (Fig. 2b,c) and group-averaged maps (Fig. 3b,c), strong response modulations were observed in the foveal and peripheral surround regions. These reflected responses evoked by the surround component directly. In addition to these surround responses, response modulations in opposite phase to the surround responses were observed within regions centered on the test regions in V1 and V2. The responses at this region increased when the surround was absent and decreased when the surround was present, indicating that the surround suppressed the response to the test. The comparison of iso- and cross-orientation suggests that the magnitude of the suppression was stronger for iso-orientation than for cross-orientation.

The suppression of the test responses was therefore dependent on the relative orientation of the test and the surround. The orientation selectivity of the suppression was examined in detail in the next series of experiments.

To quantify the magnitude of the suppression and its spatial distribution for each stimulus condition, we computed the modulation amplitude of each iso-eccentricity band in a group-averaged map from the amplitude and phase of the stimulus frequency component (Fig. 4). The estimated modulation amplitude was plotted as a function of cortical distance (from peripheral to foveal region). Figure 4b,c shows that test responses were reduced in the presence of the iso- and cross-oriented surround in V1 and V2 but not in V3/VP. In V1 and V2, significant suppressive modulation was observed in narrow regions around the test center, which was about 7 mm distant from the test-surround boundary. These modulation patterns also indicated about 3-mm surround response spread into

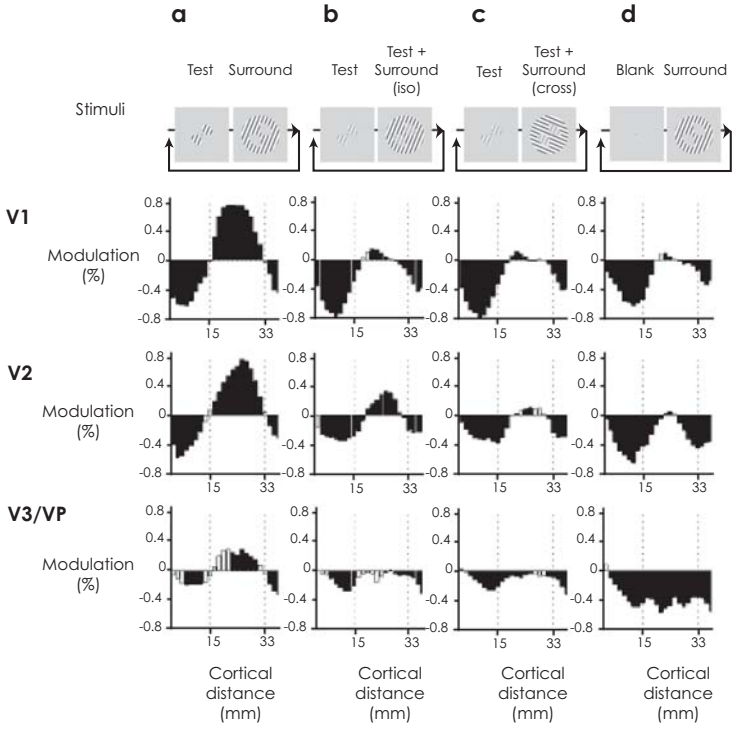

FIG. 4. Distribution of response modulations as a function of cortical distance from the 16° eccentricity line. Positive denotes that the response in the test-block was stronger than in the with-surround block, when the surround was presented. *Bars* show statistically significant modulations (Fourier F test, $P < 1e^{-4}$). **a** Results for localizer condition. **b** Results for iso-oriented surround condition. **c** Results for cross-oriented surround condition. **d** Results for control condition

the test region, which could cancel out the suppressive modulation of the test responses near the test-surround boundary.

2.1.3. Surround Modulation in the Absence of Test

In a separate control scan, we assessed whether surround suppression could be observed if the test was absent. If suppression was silent or much weaker in the absence of the test than in the presence of the test, it is likely that suppression is mediated by the interaction beyond Classified Receptive Field (CRF) (silent inhibition). We tested this by presenting a surround component in only one of the two 16-s blocks (test was not presented in both blocks).

The magnitude of the suppressive modulations without the test component in each area (Figs. 3d, 4d) was weaker than for the iso-orientation stimulus with the test (Figs. 3b, 4b), although it was similar to the cross-orientation stimulus (Figs. 3c and 4c). Thus, modulation without test, which might reflect the suppression of baseline activity in the test region or hemodynamic stealing uncorrelated with neural activity, was too weak to account for suppressive modulation, especially for the iso-orientation condition. Hence, we concluded that interaction beyond CRF predominantly contributes to suppression by the surround, at least for the iso-orientation condition.

Figures 3d and 4d show that surround responses in V3/VP spread into the center of the test region, probably because of relatively large CRFs (Smith et al. 2001). In V1 and V2, the spread of the surround response was limited to a smaller region near the test-surround boundary. The wide spread of response in V3/VP may explain why surround suppression of the test response was not evident in V3/VP, as shown in Figs. 3bc and 4bc. For our stimulus setting, suppressive modulations in the test region were likely to be largely canceled out by the spread surround responses. Cancellation by the spread surround response implies that the apparent magnitude of the suppression would depend on the size of CRF, the size of the stimulus, and spatial resolution of the measurement. If a larger stimulus was used, suppression might be observed in V3/VP. Conversely, if the modulations were measured in coarser spatial resolution, for instance, using large regions of interest (ROIs) such as the whole test region shown in Fig. 3a, modulation in the presence of the surround in V1 and V2 might be underestimated.

2.2. Orientation Selectivity of Lateral Interaction: Iso-Orientation Versus Cross-Orientation

In the second series of experiments, we compared responses to iso- and cross-orientation stimuli directly using a block-design paradigm to examine further the orientation selectivity of the surround suppression. The iso- and cross-orientation stimuli used in experiment 1 were presented in alternating 16-s blocks; hence, only the relative orientations of the test and surround gratings were changed between the blocks. We expected that the response in the test region would be stronger for the cross-orientation stimulus because iso-oriented surround sup-

presses the test response more strongly than cross-oriented surround. We also made measurements with mirror-symmetrical stimuli (test components in the lower right and upper left quadrants of the visual field) to test interhemisphere asymmetry.

We observed robust response modulations that were phase locked to the change in relative orientation of the test and surround. Figures 5 and 6 show group-averaged results. The responses in the test regions increased for the cross-orientation stimulus and decreased for the iso-orientation stimulus. The modulations were statistically significant in the test region for V1, V2, and V3/VP (Fig. 6a); thus, as expected, the test regions responded more strongly to the cross- than the iso-orientation stimulus. The modulations were also statistically significant for the mirror-symmetrical stimuli (Figs. 5b, 6b), indicating no interhemisphere asymmetry. These results supported that suppression of the test responses was stronger with the iso-oriented surround than the cross-oriented surround in V1 and V2, as suggested by the results of experiment 1. The results also suggested that similar orientation-selective modulation also occurred in V3/VP, which did not show the clear existence of surround suppression in experiment 1.

Note here that the spatial pattern of the response modulation in Figs. 5a,b and 6a,b reflects the configuration of the test and the surround. Interestingly, we

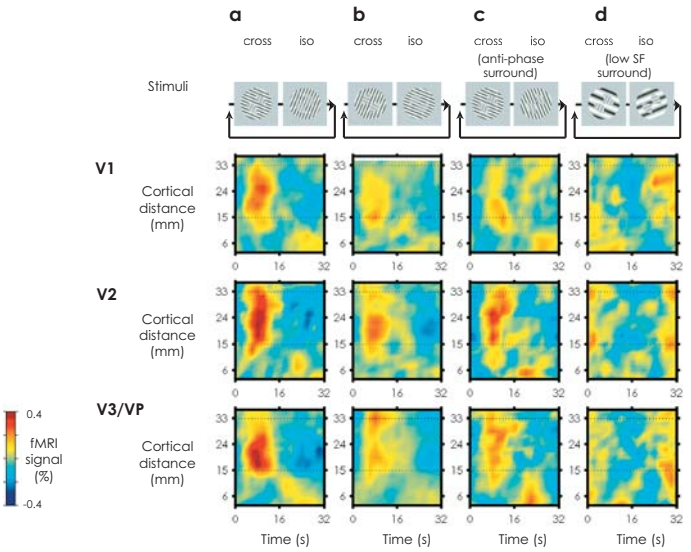

FIG. 5. Group-averaged spatiotemporal maps of V1, V2, and V3/VP to alternation of the cross- and the iso-orientation stimuli. **a** Results for the surround of the same spatial frequency and phase as the test (iso-phase surround condition). **b** Results for mirror-symmetrical iso-phase stimuli. **c** Results for the surround of the same spatial frequency but in antiphase (antiphase surround condition). **d** Results for the surround of low spatial frequency (low-SF surround condition)

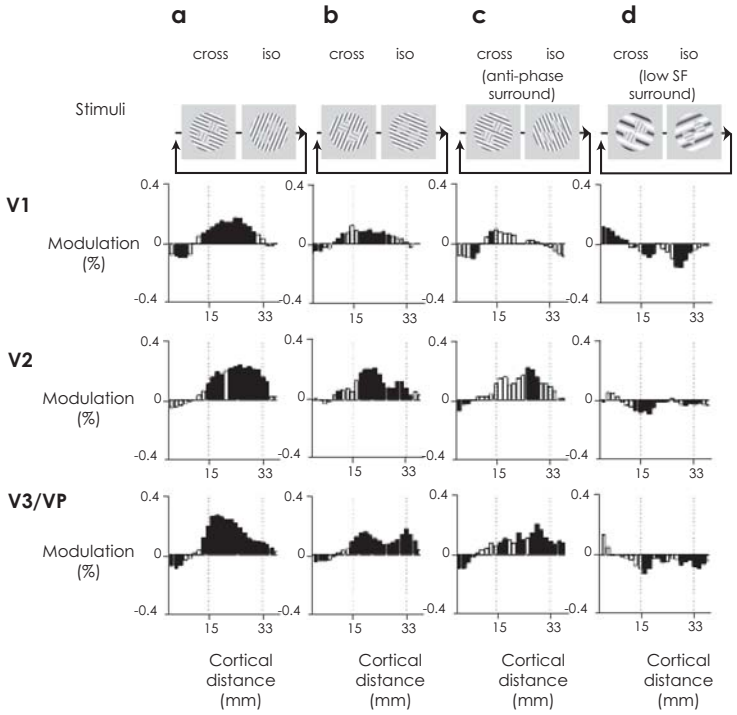

FIG. 6. Distribution of response modulations to alternation of the cross- and the iso-orientation stimuli. **a** Results for the iso-phase surround condition. **b** Results for the mirror-symmetrical stimuli. **c** Results for antiphase surround condition. **d** Results for low-SF surround condition

observed modulation in the surround regions, which were in reverse relationship with those in the test regions (that is, decrease for the cross-orientation stimulus and increase for the iso-orientation stimulus). The magnitude of suppressive (positive) modulation tended to peak at the center of the test region, and the modulation reversed across the boundaries. This finding means that not only the response to the test component but also that to the high-contrast surround component could be modulated depending on the relative orientation; this suggests that lateral interaction could be antagonistic between the test and surround regions.

Although an antagonistic pattern of modulations was observed in many cases, in some cases the modulations peaked at the test-surround boundary and reduced as the distance from the boundary increased. This spatial pattern of response could be well explained by the local responses to feature contrast at the boundary (Kastner et al. 1997; Knierim and Van Essen 1992). It can be argued that the local responses could spread into the center of the test region, resulting in an apparent peak, especially for areas with larger CRF. According to our result

shown in Fig. 3d and the estimation of cortical point spread function (Engel et al. 1997), V3/VP is likely to be such a case for our stimulus, but V1 and V2 are not, as the spread in V1 and V2 was likely to be much smaller than the distance between the test-surround boundary and the center of the test region. Hence, although the responses to local feature contrast at the boundary are potential sources of response modulation around the test region, the contribution of these local responses to V1 and V2 was not dominant for our stimulus.

2.3. *Effect of Relative Spatial Frequency and Phase*

Finally, we manipulated the spatial frequency and phase of the surround grating and examined how these affected the response modulations for the iso- and cross-orientation. We used two conditions, an antiphase surround condition, in which the test and surround differed in the spatial phase, and a low spatial frequency (low-SF) surround condition, in which the test and surround differed by more than a octave in spatial frequency (0.66 cpd for the surround, 2.0 cpd for the test). According to psychophysical literature, these manipulations could affect subjects' perception. Our subjects reported that the apparent contrast of the test was slightly lower for iso-orientation than cross-orientation even when the test and surround differed in the spatial phase (antiphase surround condition), but not when they differed in spatial frequency (low-SF surround condition). The results showed that the antiphase surround produced suppressive response modulations in the test region for V2 and V3/VP (Figs. 5c, 6c) but was not statistically significant for V1. Suppressive response modulations were not observed in any areas in the low-SF surround condition (Figs. 5d, 6d). These tendencies were in accordance with the effects of these parameters on perceptual contrast.

2.4. *Origin of Surround Suppression*

The suppressive interaction observed in this study agrees with recent fMRI and Magnetoencephalography (MEG) studies that showed suppressive interaction among nearby stimuli in human early visual areas (Kastner et al. 1998, 2001; Ohtani et al. 2002; Zenger-Landolt and Heeger 2003). Kastner et al. (1998, 2001) have reported a suppressive effect that was analogous to "sensory suppression" within CRF at the level of a single neuron. Note that the surround suppression observed in our study was selective to the relative orientation of the test and surround, whereas sensory suppression is not; thus the observed surround suppression is not simply sensory suppression. The relative-orientation-selective surround suppression observed in our study is analogous to the response modulation beyond CRF that was found at the level of a single neuron in the cat and monkey primary visual cortex. For contrast parameters similar to ours, the iso-oriented surround presented outside CRF markedly suppressed neuronal response to a stimulus in CRF, while cross-oriented surround had a weak effect or none (Levitt and Lund 1997). Similar relative orientation-selective surround

suppression has also been found by optical imaging of cat area 17 (Toth et al. 1996), indicating that surround suppression beyond CRF could be observed in a large population of neurons. Our finding that surround suppression was weakened in the absence of the test also supported the contribution of the interaction beyond CRF. Hence, the surround suppression observed in our study reflects, in part, context-dependent suppression mediated by the interaction beyond CRFs.

3. Generating Meanings from Ambiguous Visual Inputs

Psychological projective tests, such as the Rorschach inkblot test, have a long history of use as mental assessments. This method requires respondents to construct meanings based on ambiguous patterns. Although there is controversy surrounding the projective tests, the Rorschach inkblot test is considered to be valid for identifying schizophrenia and other disturbances marked by disordered thoughts. A neuroimaging study on the generation of fluent speech during the Rorschach inkblot test focused on the brain activity in the superior temporal cortex, and showed that patients with formal thought disorders showed a reversed laterality of activation in the superior temporal cortex (Kircher et al. 2000). There are few data on the specific brain areas that are involved in semantic processing of visual inputs during the Rorschach test because the temporal cortex may be involved in the word generation process. Generation of meanings from ambiguous visual patterns may result from interactions between memory and perception. An electroencephalographic (EEG) investigation (Gill and O'Boyle 2003) showed that, when naming inkblot stimuli, bilateral activation of the parietal and occipital lobes was initiated and complemented by activation of the right frontal lobe, suggesting anterior regions of the right cerebral hemisphere contribute to the generation of meanings from visually ambiguous patterns. Identifying the brain areas that are involved in generation of meaning independent of word generation would further delineate meaning-related functions within the brain.

To assess meaning-related brain activity, we employed a naming task in which subjects were asked to name each of the visual stimuli covertly, as many as possible, while regional blood oxygen-action level-dependent (BOLD) contrast was measured using fMRI.

Figure 7a shows the visual materials employed. Three types of stimuli were used: five Rorschach inkblots (Cards I, IV, V, VI, and VII), five geometric shapes, and five face-like patterns. Rorschach inkblots and geometric figures were ambiguous, but their shapes provoked semantic associations with various categories, such as faces, particular animals, and so on. All were black- and white-figures ($8.4° \times 8.4°$; $240\,cd/m^2$ for white). We used the event-related paradigm: each of the visual stimuli was presented with a duration of 15 s followed by a 21-s uniform field with a fixation point; five stimuli of each stimulus type were presented in the order shown in Fig. 7a within one session, and two sessions were run for each stimulus type. In the naming task, subjects were asked to think "what this might be" and to name covertly, for each stimulus, as many items as possible.

No overt response, such as a verbal response or key press, was required, but subjects were required to assign as many names as possible. As a control experiment, we carried out fMRI measurements during passive viewing of the stimuli: subjects were instructed to concentrate on fixating on the central part of the stimulus and not to think about the visual stimuli.

All imaging used a General Electric 1.5-tesla scanner. The data were analyzed and visualized using our own in-house software (Ejima et al. 2003). The three-dimensional cortical surface was reconstructed for each. The reconstructed cortical surface was transformed into stereotaxic space (Talairach and Tournoux 1988). The fMRI data were processed using a temporal correlation analysis (Bandettinni et al. 1993). The linear trend and baseline offset for each voxel time series were first removed. A reference waveform was modeled with stimulus-related activation as a delayed "boxcar" function, taking into account the hemodynamic response lag convolved by a gamma function (phase delay = 3, pure delay = 2.5 s, time constant = 1.25 s) (Boynton et al. 1996). We employed an empirical procedure proposed by Baudewig et al. (2003), which introduced thresholds as *P* values and defined thresholds with respect to the physiological noise distribution of individual statistical parametric maps. In the first step, a histogram of correlation coefficients, calculated using the reference functions, was used to estimate the underlying noise distribution of individual correlation images. In the second step, a Gaussian curve was fitted to the central portion of the histogram. In the third step, the distribution of correlation coefficients was rescaled into percentile ranks of the individual noise distribution. The percentile rank of 99.99% ($P = 0.0001$) served as the threshold for the identification of activation voxels. Voxels were deemed activated if they had a correlation coefficient greater than the threshold correlation coefficient defined by the *P* value of 0.0001. We conducted an analysis in anatomically defined ROIs for the prefrontal, parietal, and occipital cortex. Ten ROIs were defined as regions within each gyrus, taking account of the anatomical structure and Brodmann areas (BAs) for each of the reconstructed cortical surfaces (Damasio 1990). Ten ROIs for the right hemisphere of one subject are shown in Fig. 8a. We sampled the fMRI data set from the full area of each ROI. Voxels within each region reaching a voxel threshold of $P < 0.0001$ were counted.

Behaviorally, in the naming task, the subjects reported that they assigned a much larger number of different names to the Rorschach inkblots and the geometric shapes than to the face-like stimuli, to which almost all subjects assigned one or two names. The regions of stimulus-related activation at the $P = 0.0001$ significance threshold were localized on the cortices of six subjects. Generation of meanings from ambiguous patterns resulted in extensive activation in regions including the prefrontal, parietal, and occipital cortex. Figure 7b shows brain activity for the Rorschach inkblots mapped on the reconstructed surface from the left and right hemispheres of one representative subject. Orange-yellow denotes the voxel locations activated during a naming task, and the colors represent *P* values above 0.0001. Dark-blue-blue denotes the voxel locations activated during passive viewing, and the colors represent the *P* values above 0.0001.

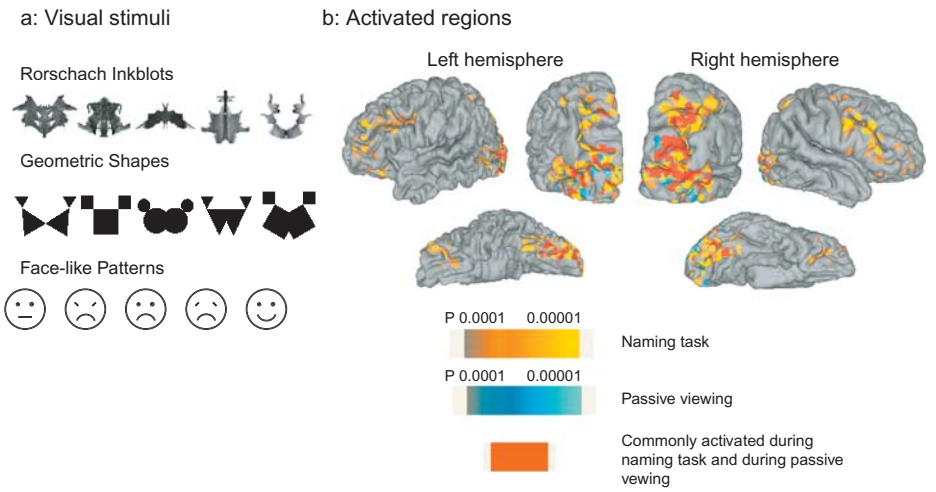

FIG. 7. **a** Visual stimuli employed in the experiment. **b** Activation maps for the naming task and the baseline (passive viewing). Areas selectively activated ($P < 0.0001$) are mapped on the reconstructed surface from the left and right hemispheres of one representative subject. Three views (lateral, posterior, and ventral) are presented. The visual stimuli were Rorschach inkblots. *Orange-yellow colors* denote the cortical regions showing significant activation during the naming task. The colors represent P values above 0.0001. *Dark-blue-blue colors* denote cortical regions showing significant activation during passive viewing. The colors represent P values above 0.0001. *Red* denotes the cortical regions showing significant activation common during the naming task and passive viewing

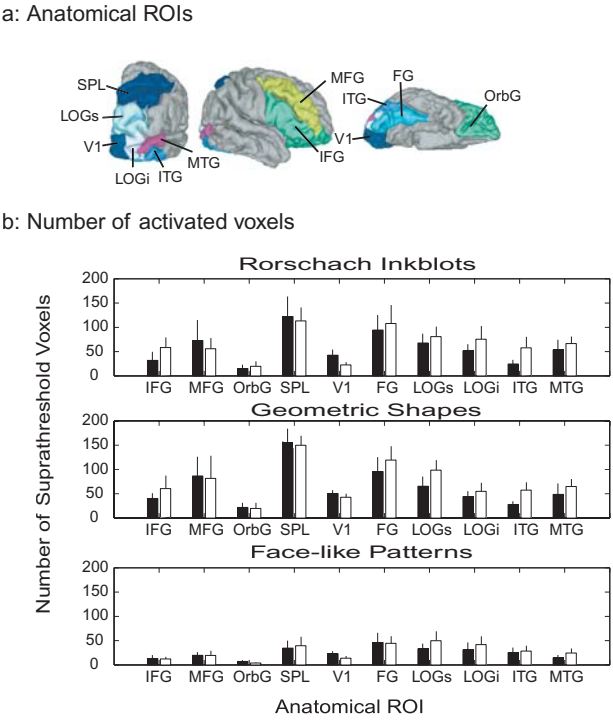

TABLE 1. Activation loci in the prefrontal cortex during naming task

	Left hemisphere coordinates			Right hemisphere coordinates		
	x	*y*	*z*	*x*	*y*	*z*
Anterior MFG (BA46)	–35 (8)	45 (9)	19 (7)	37 (3)	47 (6)	7 (9)
Mid-MFG (BA9)	–41 (5)	29 (10)	29 (5)	41 (6)	35 (7)	20 (8)
Posterior MFG (BA8)	–45 (2)	20 (10)	33 (6)	39 (7)	21 (5)	35 (8)
Anterior IFG (BA45)	–41 (8)	42 (13)	13 (8)	46 (2)	37 (5)	6 (7)
Posterior IFG (BA44)	–46 (4)	23 (10)	22 (4)	48 (3)	29 (6)	15 (7)
Orbitofrontal gyrus (BA11)						
Anterior	–24 (7)	46 (9)	–15 (4)	26 (5)	49 (3)	–15 (3)
Posterior	–29 (6)	34 (8)	–15 (5)	28 (3)	35 (3)	–16 (4)

The numbers in parentheses denote ± standard error of mean; $n = 6$
MFG, middle frontal gyrus; *IFG*, inferior frontal gyrus

Red denotes the voxel locations activated commonly during the naming task and passive viewing. A similar activation pattern was observed for the geometric shapes. Multiple, bilateral regions in the prefrontal cortex were activated; these included bilateral prefrontal activation in the cortical areas lining the inferior frontal sulcus (IFS), middle frontal gyrus (MFG, BA46/8/9), and inferior frontal gyrus (IFG, BA44/45). The clustering in the lateral prefrontal activations was similar among subjects. There were foci of activity within the orbitofrontal cortex (OrbFC, BA11). The foci lay along the rostral and caudal parts of the lateral orbital sulcus. On the medial surface, we observed no significant consistent activation among subjects, and we did not observe significant activation in the anterior cingulated cortex.

Table 1 shows the means of the Talairach coordinates of the activated regions in the prefrontal cortex across six subjects. These regions showed consistent

FIG. 8. **a** Ten anatomical regions of interest (ROIs) defined on the reconstructed surface (right hemisphere) of one subject. *MFG*, middle frontal gyrus; *IFG*, inferior frontal gyrus; *OrbG*, orbitofrontal gyri; *SPL*, superior parietal lobule; *LOGs*, superior part of lateral occipital gyri; *LOGi*, inferior part of lateral occipital gyri; *MTG*, middle temporal gyrus; *ITG*, inferior temporal gyrus; *FG*, fusiform gyrus; *V1*, area surrounding the calcarine sulcus including the lingual gyrus. **b** The number of suprathreshold voxels within each anatomical ROI, averaged across six subjects. The graph represents the number (± standard error of mean) of suprathreshold voxels ($P < 0.0001$) within ten ROIs. *Black columns* = left; *white columns* = right. Data are for the naming task: *top* for Rorschach inkblots, *middle* for geometric shapes, and *bottom* for face-like patterns

activation across all subjects. During passive viewing, we did not observe activation in the regions of the prefrontal cortex. During the naming task, besides the prefrontal cortex, extensive activation was observed in the parietal (SPL), temporal (MTG, ITG), ventral (FG), and occipital (superior LOG, inferior LOG, V1) cortices. These regions were also activated during passive viewing, denoted by red and blue colors in Fig. 7b. Note that the activation in these regions during the naming task extended around the loci of activation observed during passive viewing, denoted by commonly activated voxels, and denoted by red in Fig.7b. We also found that the amplitude of the fMRI signals in commonly activated regions was larger for the naming task than for the passive viewing.

Brain activation strongly depended on the ambiguity and/or stimulus characteristics of visual inputs. Figure 8b shows the number of suprathreshold voxels ($P < 0.0001$) within each of ten anatomical ROIs, averaged across six subjects for three stimulus types for the naming task. For face-like patterns, the number of activated voxels was markedly reduced for all the anatomical ROIs, comparing the data for the ambiguous patterns. There were some asymmetries between hemispheres in the activation, as measured by the number of suprathreshold voxels. All six subjects had more suprathreshold voxels in the inferior temporal gyrus (ITG) on the right than the left. There was significant right-sided asymmetry for the whole group ($t(6) = 3.15$, $P < 0.025$ for the geometric shapes; $t(6) = 2.65$, $P < 0.045$ for the Rorschach inkblots). There were more suprathreshold voxels within the right IFG, LOG, FG, and MTG than the left. On the other hand, there were more suprathreshold voxels in the left MFG and SPL than the right. The laterality effects, however, were not statistically significant ($P > 0.05$). The asymmetries in activation were not absolute: the naming task resulted in suprathreshold voxels bilaterally, but the relative ratio differed according to the cortical regions.

We adopted a covert procedure in which subjects generated names silently and found the activation pattern was very similar to that obtained by fMRI study of perceptual categorization (De Beek et al. 2000; Vogels et al. 2002) using a variant of the well-known dot pattern classification. The activated brain regions shown in the present study show the perceptual-conceptual memory system for visual inputs in the brain proposed in the literature. There are converging lines of evidence suggesting that conceptual and perceptual memory processes are subserved by different parts of the brain; regions in the inferior frontal gyrus, middle temporal gyrus, and inferior temporal gyrus are involved in conceptual memory processes, whereas the occipital cortex is involved in the perceptual memory process for visual stimuli and the superior temporal gyrus is involved in perceptual memory for auditory stimuli (Blaxton 1999; Buckner et al., 2000). We also found that the activation regions involved SPL and a part of the frontal eye field situated just behind the dorsolateral frontal region. These regions are known to be involved in processing spatial information in the visually guided saccade (Merriam et al. 2001). Eye tracking dysfunction is one of the established markers of risk for schizophrenia (Clementz and Sweeney 1990; Sweeney et al. 1998). The present study suggests that eye movement abnormalities observed for schizo-

phrenia during the Rorschach inkblot test (Fukuzako et al. 2002) are likely caused by the abnormalities in these brain regions.

Acknowledgment. We appreciate the assistance of C. Tanaka, K.M. Fukunaga, T. Ebisu, and M. Umeda with fMRI. This study was supported by the 21st Century COE Program (D-2, Kyoto University) from the Ministry of Education, Culture, Sports, Science and Technology, Japan.

References

Bandettini PA, Jesmanowicz A, Wong EC, Hyde JS (1993) Processing strategies for time-course data sets in functional MRI of the human brain. Magn Reson Med 30:161–173

Baudewig J, Dechent P, Merboldt KD, Frahm J (2003) Thresholding in correlation analyses of magnetic resonance functional neuroimaging. Magn Reson Imag 21:1121–1130

Blaxton T (1999) Cognition: memory, 2. Conceptual and perceptual memory. Am J Psychiatry 156:1676

Boynton GM, Engel SA, Glover GH, Heeger DJ (1996) Linear systems analysis of functional magnetic resonance imaging in human V1. J Neurosci 16:4207–4221

Buckner RL, Koutstaal W, Schacter DL, Rosen BR (2000) Functional MRI evidence for a role of frontal and inferior temporal cortex in amodal components of priming. Brain 123:620–640

Cannon MW, Fullenkamp SC (1991) Spatial interactions in apparent contrast: inhibitory effects among grating patterns of different spatial frequencies, spatial positions and orientations. Vision Res 31:1985–1998

Clementz BA, Sweeney JA (1990) Is eye movement dysfunction a biological marker for schizophrenia? A methodological review. Psychol Bull 108:77–92

Damasio H (1990) Human brain anatomy in computerized images. Oxford University Press, New York

De Beek HO, Beatse E, Wagemans J, Sunaert S, Hecke P (2000) The representation of shape in the context of visual object categorization tasks. Neuroimage 12:28–40

Ejima Y, Takahashi S (1985) Apparent contrast of a sinusoidal grating in the simultaneous presence of peripheral gratings. Vision Res 25:1223–1232

Ejima Y, Takahashi S, Yamamoto H, Fukunaga M, Tanaka C, Ebisu T, Umeda M (2003) Interindividual and interspecies variations of the extrastriate visual cortex. NeuroReport 14:1579–1583

Engel SA, Glover GH, Wandell BA (1997) Retinotopic organization in human visual cortex and the spatial precision of functional MRI. Cereb Cortex 7:181–192

Engel SA, Rumelhart DE, Wandell BA, Lee AT, Glover GH, Chichilnisky, EJ, Shadlen MN (1994) fMRI of human visual cortex. Nature (Lond) 369:525

Fukuzako H, Sugimoto H, Takigawa M (2002) Eye movements during the Rorschach test in schizophrenia. Psychiatry Clin Neurosci 56:409–418

Furmanski CS, Engel SA (2000) An oblique effect in human primary visual cortex. Nat Neurosci 3:535–536

Gill HS, O'Boyle MW (2003) Generating an image from an ambiguous visual input: an electroencephalographic (EEG) investigation. Brain Cognit 51:287–293

Kastner S, Nothdurft H, Pigarev IN (1997) Neuronal correlates of pop-out in cat striate cortex. Vision Res 37:371–376

Kastner S, De Weerd P, Desimone R, Ungerleider LG (1998) Mechanisms of directed attention in the human extrastriate cortex as revealed by functional MRI. Science 282:108–111

Kastner S, De Weerd P, Pinsk MA, Elizondo MI, Desimone R, Ungerleider LG (2001) Modulation of sensory suppression: implications for receptive field sizes in the human visual cortex. J Neurophysiol 86:1398–1411

Kircher TTJ, Brammer MJ, Williams SCR, McGuire PK (2000) Lexical retrieval during fluent speech production: an fMRI study. NeuroReport 11:4093–4096

Knierim JJ, Van Essen DC (1992) Neuronal responses to static texture patterns in area V1 of the alert macaque monkey. J Neurophysiol 67:961–980

Lamme VAF (1995) The neurophysiology of figure-ground segregation in primary visual cortex. J Neurosci 15:1605–1615

Levitt JB, Lund JS (1997) Contrast dependence of contextual effects in primate visual cortex. Nature (Lond) 387:73–76

Merriam EP, Colby CL, Thulborn KR, Luna B, Olson CR, Sweeney JA (2001) Stimulus-response incompatibility activates cortex proximate to three eye fields. Neuroimage 13:794–800

Ohtani Y, Okamura S, Yoshida Y, Toyama K, Ejima Y (2002) Surround suppression in the human visual cortex: an analysis using magnetoencephalography. Vision Res 42:1825–1835

Reynolds JH, Chelazzi L, Desimone R (1999) Competitive mechanisms subserve attention in macaque areas V2 and V4. J Neurosci 19:1736–1753

Sereno MI, Dale AM, Reppas JB, Kwong KK, Belliveau JW, Brady TJ, Rosen BR, Tootell RB (1995) Borders of multiple visual areas in humans revealed by functional magnetic resonance imaging. Science 268:889–893

Sillito AM, Grieve KL, Jones HE, Cudeiro J, Davis J (1995) Visual cortical mechanisms detecting focal orientation discontinuities. Nature (Lond) 378:492–496

Smith AT, Singh KD, Williams AL, Greenlee MW (2001) Estimating receptive field size from fMRI data in human striate and extrastriate visual cortex. Cereb Cortex 11: 1182–1190

Sweeney JA, Luna B, Srinivasagam NM, Keshavan MS, Schooler NR, Haas GL, Carl JR (1998) Eye tracking abnormalities in schizophrenia: evidence for dysfunction in the frontal eye field. Biol Psychiatry 44:698–708

Takeuchi T, De Valois KK (2000) Modulation of perceived contrast by a moving surround. Vision Res 40:2697–2709

Talairach J, Tournoux P (1988) Co-planar stereotaxic atlas of the human brain. Thieme, New York

Toth TJ, Rao SC, Kim DS, Somers D, Sur M (1996) Subthreshold facilitation and suppression in primary visual cortex revealed by intrinsic signal imaging. Proc Natl Acad Sci U S A 93:9869–9874

Vogels R, Sary G, Dupont P, Orban GA (2002) Human brain regions involved in visual categorization. Neuroimage 16:401–414

Woods RP, Cherry SR, Mazziotta JC (1992) Rapid automated algorithm for aligning and reslicing PET images. J Comput Assist Tomogr 16:620–633

Xing J, Heeger DJ (2000) Center-surround interactions in foveal and peripheral vision. Vision Res 40:3065–3072

Zenger-Landolt B, Heeger DJ (2003) Response suppression in V1 agrees with psychophysics of surround masking. J Neurosci 23:6884–6893

Zipser K, Lamme VAF, Schiller PH (1996) Contextual modulation in primary visual cortex. J Neurosci 16:7376–7389

2
Multiple Mechanisms of Top-Down Processing in Vision

Giorgio Ganis[1,2,3] and Stephen M. Kosslyn[3,4]

1. Introduction

No animal could survive for long without perception. We must perceive the world, not only to find food, shelter, and mates, but also to avoid predators. Perception will fail if an animal does not register what is actually in the world. However, this simple observation does not imply that all processing during perception is "bottom up"—driven purely by the sensory input. Rather, bottom-up processing can be usefully supplemented by using stored information, engaging in processing that is "top down"—driven by stored knowledge, goals, or expectations. In this chapter we explore the nature of top-down processing and its intimate dance with bottom-up processing. We begin by considering basic facts about the primate visual system, and then consider a theory of its functional organization, followed by novel proposals regarding the nature of different sorts of top-down processing.

2. The Structure of Visual Processing in the Brain

An enormous amount has been learned about visual processing by studying animal models. In particular, the macaque monkey has very similar visual abilities to those of humans, and the anatomy of its visual system appears very similar to ours. Studies of the monkey brain have revealed key aspects of the organization of the visual system, namely, its hierarchical structure and the reciprocal nature of most connections between different visual areas of the brain. We briefly review key aspects of both characteristics of the brain next.

[1]Department of Radiology, Harvard Medical School, Boston, MA 02115, USA
[2]Massachusetts General Hospital, Martinos Center, Charlestown, MA 02129, USA
[3]Department of Psychology, Harvard University, Cambridge, MA 02138, USA
[4]Department of Neurology, Massachusetts General Hospital, Boston, MA 02142, USA